Available online at www.sciencedirect.com
ScienceDirect
Journal of Power Sources 171 (2007) 932–937
JOURNAL OF POWER SOURCES
www.elsevier.com/locate/jpowsour

Short communication

Charge/discharge behavior of plasma-fluorinated natural graphites in propylene carbonate-containing solvent

Takashi Achiha [a], Seiko Shibata [a], Tsuyoshi Nakajima [a,*], Yoshimi Ohzawa [a], Alain Tressaud [b], Etienne Durand [b]

[a] *Department of Applied Chemistry, Aichi Institute of Technology, Yakusa, Toyota 470-0392, Japan*
[b] *ICMCB-CNRS, Université Bordeaux I, 87 Ave. Dr. A. Schweitzer, 33608 Pessac, France*

Received 4 April 2007; received in revised form 2 June 2007; accepted 6 June 2007
Available online 13 June 2007

Abstract

Plasma-fluorination of natural graphite samples with average particle sizes of 5 μm, 10 μm and 15 μm (NG5μm, NG10μm and NG15μm) was performed using CF_4 and charge/discharge characteristics of surface-fluorinated samples were investigated in 1 mol dm^{-3} $LiClO_4$–ethylene carbonate (EC)/diethyl carbonate (DEC)/propylene carbonate (PC) (1:1:1, v/v/v). Fluorine contents obtained by elemental analysis were in the range of 0.3–0.6 at.% and surface fluorine concentrations determined by X-ray photoelectron microscopy (XPS) were 14.8–17.3 at.%. Plasma-fluorination increased surface disorder of natural graphite samples though reduced surface areas due to its surface etching effect. Electrochemical decomposition of PC was highly reduced on surface-fluorinated NG10μm and NG15μm with high disorder. First coulombic efficiencies of plasma-fluorinated NG10μm and NG15μm increased by 9.7 and 19.3% at 150 mA g^{-1}, respectively.

Keywords: Plasma-fluorination; Surface modification; Graphite anode; Lithium ion battery

1. Introduction

Graphitic materials such as natural and synthetic graphites with high crystallinity are mainly used as anodes of lithium ion batteries in combination with ethylene carbonate (EC)-based solvents. Graphite has several advantages of low electrode potential, small irreversible capacity (high first coulombic efficiency), good cycleability and constant capacity. Natural graphite shows high reversible capacity (∼360 mAh g^{-1}) close to the theoretical discharge capacity (372 mAh g^{-1}) while synthetic graphite often gives slightly lower capacity than natural graphite because of its lower crystallinity. It is well known that EC-based solvents should be employed for graphite anode with high crystallinity for the quick formation of protective surface film (solid electrolyte interface, SEI) with decomposition of a small amount of EC [1]. EC has, however, a high melting point of 36 °C. Therefore the use of propylene carbonate (PC) with a low melting point of −55 °C is desirable for graphite anode. It is unfortunately difficult to use PC-based solvents for graphite since electrochemical reduction of PC vigorously occurs on graphite. It is also known that PC can be used for low crystalline carbons having higher surface disorder than graphite. It suggests that high crystalline graphite may be used in PC-based solvents if surface disordering is attained by surface modification. Surface modification is one of the effective methods for improving electrode characteristics of carbonaceous anodes. Recently various methods of surface modification were reported [2–4]. They include carbon coating [5–13], metal or metal oxide coating [14–20], surface oxidation [21–27], surface fluorination [28–40] and polymer or Si coating [41–47]. These methods improved such electrode characteristics of carbonaceous anodes as reversible capacities, first coulombic efficiencies (irreversible capacities), cycleability and so on. Among them, surface fluorination is effective for improving the electrochemical behavior of graphitic materials. When low crystalline carbons are fluorinated by fluorinating gases, carbon–carbon bond rupture leading to the formation of gaseous fluorocarbons such as CF_4 easily occurs. However, surface-fluorinated layers with covalent C–F bond are formed when natural or synthetic graphite is fluorinated. Fluorination mechanisms of carbon materials are different

* Corresponding author. Tel.: +81 565 48 8121x2201; fax: +81 565 48 0076.
E-mail address: nakajima-san@aitech.ac.jp (T. Nakajima).

0378-7753/$ – see front matter © 2007 Elsevier B.V. All rights reserved.
doi:10.1016/j.jpowsour.2007.06.008

depending on fluorinating agents or fluorination techniques. Fluorination of graphite by F_2 is an electrophilic reaction in which $F^{\delta+}$ preferentially attacks carbon atom with higher electron density ($C^{\delta-}$) and $F^{\delta-}$ reacts with $C^{\delta+}$, yielding fluorinated layers with C–F covalent bond [48–50]. Surface fluorination of natural graphites and graphitized petroleum cokes by F_2 gave fluorinated layers with high disorder [28–30,32–35,37,40]. On the other hand, the reactions of ClF_3 and NF_3 with carbon materials are radical reactions by chemically active species such as F, Cl, ClF_2 and NF_2 generated by thermal decomposition of ClF_3 and NF_3 [36,37,39]. Plasma-fluorination using CF_4 gas is also a radical reaction by radical species such as CF_3 produced under plasma [30,31,38]. Radical reactions have surface etching effect easily producing fluorocarbon gases. In fact, no surface fluorine was detected and no increase in surface disorder was observed when graphitized petroleum cokes were fluorinated by ClF_3 and NF_3 at 200–500 °C [36,37]. However, fluorinated layers with high disorder were formed in the surface region of high crystalline natural graphite even when fluorinated by ClF_3 at 200–300 °C because natural graphite has a strong carbon skeleton [39]. Plasma-fluorination also gave fluorinated layers with high disorder for both natural graphite and graphitized petroleum cokes probably because the sample temperature was low, i.e., 90 °C [30,31,38]. Surface disorder of graphitized petroleum cokes was enhanced by the surface fluorination with F_2 [33–35], and plasma-fluorination using CF_4 [38]. The increase in surface disorder of graphitized petroleum cokes led to decrease in their irreversible capacities, i.e., increase in first coulombic efficiencies in EC-based solvent [33–35]. In the case of high purity natural graphite samples with large surface areas, surface disorder was increased by the fluorination not only with F_2 [40] but also with ClF_3 [39]. Electrochemical reduction of PC was highly reduced on the surface-fluorinated samples, which led to large increase in first coulombic efficiencies in PC-containing solvent [39,40]. In the present study, natural graphite samples with large surface areas were fluorinated by plasma-treatment using CF_4, and effect of surface fluorination on the charge/discharge behavior was investigated in PC-containing solvent.

2. Experimental

2.1. Plasma-fluorination and characterization of natural graphite samples

Raw materials were natural graphite powder samples with average particle sizes of 5 μm, 10 μm and 15 μm (abbreviated to NG5μm, NG10μm and NG15μm; d_{002} = 0.3355 nm, 0.3354 nm and 0.3355 nm; purity: >99.95%) supplied by SEC Carbon Co. Ltd. Their X-ray diffraction patterns are shown in Fig. 1. Natural graphite sample was placed in the center of the chamber on the electrode connected to rf. Plasma-fluorination was made using CF_4 gas under the following conditions: CF_4 flow rate, 8 cm^3 min^{-1}; total gas pressure, 5.0 Pa; power, 80 W; plasma frequency, 13.56 MHz; sample temperature, 90 °C; plasma-treatment time, 60 min. Surface-fluorinated natural graphite samples were characterized by elemental analysis of C and F, X-ray diffractometry, X-ray photoelectron spectroscopy (XPS), surface area and meso-pore size distribution measurements using nitrogen gas, and Raman spectroscopy.

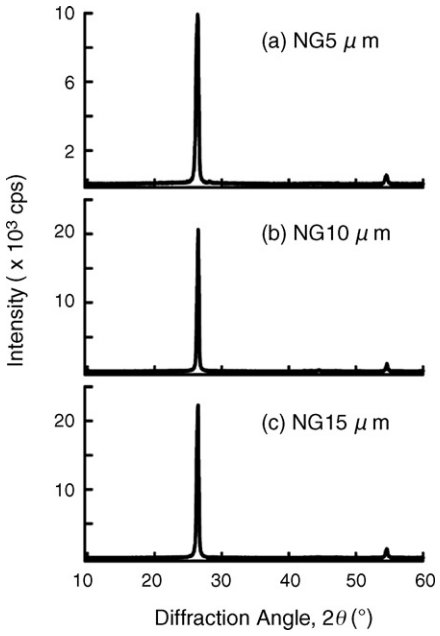

Fig. 1. X-ray diffraction patterns of (a) NG5μm, (b) NG10μm and (c) NG15μm.

2.2. Electrochemical measurement of plasma-fluorinated natural graphite samples

Three electrode-cell with natural graphite sample as a working electrode and metallic lithium as counter and reference electrodes was used for galvanostatic charge/discharge measurements. Electrolyte solution was 1 mol dm^{-3} $LiClO_4$–EC/DEC/PC (1:1:1 v/v/v). Natural graphite electrode was prepared in the following manner. Natural graphite sample was dispersed in *N*-methyl-2-pyrrolidone (NMP) containing 12 wt% poly(vinylidene fluoride) (PVdF) and slurry was pasted on a copper plate. The electrode was dried at 120 °C under vacuum overnight. After drying, the electrode contained 80 wt% natural graphite sample and 20 wt% PVdF. Charge/discharge experiments were performed at a current density of 150 mA g^{-1} between 0 and 3 V relative to Li/Li^+ in a glove box filled with Ar at 25 °C.

3. Results and discussion

3.1. Surface composition and structure of plasma-fluorinated natural graphite samples

X-ray diffraction pattern of natural graphite samples was not changed by plasma-fluorination. The change in *d*-values of (0 0 2) diffraction lines was negligible. Table 1 gives composition of plasma-fluorinated samples, obtained by elemental analysis. Fluorine content was very small, i.e., in the range of 0.3–0.6 at.% less than 1 at.%. Surface fluorine concentration obtained by XPS was in the range of 14.8–17.3 at.% (Table 2). There is no large

Table 1
Composition of plasma-fluorinated natural graphite samples, obtained by elemental analysis

Graphite sample	C (at.%)	F (at.%)	O (at.%)
NG5μm	99.3	0.6	0.1
NG10μm	99.5	0.4	0.1
NG15μm	99.7	0.3	0.0

Table 2
Surface composition of plasma-fluorinated natural graphite samples, obtained by XPS

Graphite sample	C (at.%)	F (at.%)	O (at.%)
Original			
NG5μm	91.2	–	8.8
NG10μm	91.6	–	8.4
NG15μm	90.5	–	9.5
Fluorinated			
NG5μm	75.1	17.3	7.6
NG10μm	78.5	14.8	6.7
NG15μm	77.6	15.1	7.3

difference in these data among three natural graphite samples. Surface fluorine concentrations were similar to those obtained when the same natural graphite samples were fluorinated by F_2 (3×10^4 Pa) (11.1–15.3 at.% at 200 °C and 17.7–20.5 at.% at 300 °C) [40]. When they were fluorinated by ClF_3 under the same conditions, the lower fluorine concentrations were obtained (0–6.6 at.% at 200 °C and 0.9–12.7 at.% at 300 °C) [39]. In addition, surface fluorine concentration increased with decreasing surface area, i.e., from NG5μm to NG15μm. Fluorocarbon gases such as CF_4 is mainly produced in the case of NG5μm having a large surface area since high temperature fluorination of a carbon material by ClF_3 is a radical reaction with surface etching effect [36,37,39]. Plasma-fluorination with CF_4 is also a radical reaction [30,31,38]. However, the formation reaction of fluorocarbon gases is probably slow in plasma-fluorination because the sample temperature was low, 90 °C. This may be the reason that the surface fluorine concentrations obtained in the present study are similar to those obtained when the same natural graphite samples were fluorinated by F_2. Surface oxygen was slightly reduced by plasma-fluorination in all samples.

Raman spectra of original and plasma-fluorinated natural graphite samples are shown in Fig. 2. High crystalline natural graphite powder usually shows a similar Raman spectrum. G-bands at 1580 cm^{-1} indicating graphitic structure are strong while D-bands at 1360 cm^{-1} indicating disordered structure are weak. G-bands were slightly broadened by plasma-fluorination. Table 3 gives *R*-values calculated as peak intensity ratios of

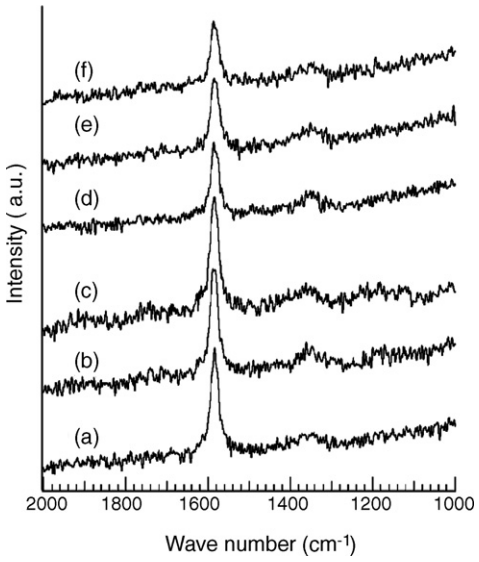

Fig. 2. Raman spectra of original and plasma-fluorinated natural graphite samples: (a) NG5μm, (b) NG10μm, (c) NG15μm, (d) plasma-fluorinated NG5μm, (e) plasma-fluorinated NG10μm and (f) plasma-fluorinated NG15μm.

D-band to G-band. *R*-values of surface-fluorinated samples were larger than those of non-fluorinated ones, increasing with increasing particle size of natural graphite, i.e., from NG5μm to NG15μm. The increase in *R*-value of NG5μm by plasma-fluorination was the same as that of NG5μm fluorinated by F_2 at 300 °C [40]. In the case of NG10μm and NG15μm, the increase in *R*-values by plasma-fluorination were also the same as those obtained for the samples fluorinated by F_2 at 200 °C, but smaller than those obtained by the fluorination with F_2 at 300 °C [40].

Table 4 gives surface areas of original and plasma-fluorinated samples. In all samples, surface areas were reduced by plasma-fluorination because plasma-fluorination is a radical reaction having surface etching effect. Fig. 3 shows meso-pore size distribution of original and plasma-fluorinated samples. Meso-pores were totally reduced by surface etching effect of plasma-fluorination, however, those with diameters of 1.5–2 nm were increased by breaking of carbon–carbon bonds.

3.2. Charge/discharge characteristics of plasma-fluorinated natural graphite samples in 1 mol dm^{-3} $LiClO_4$–EC/DEC/PC (1:1:1 v/v/v)

Degree of surface disorder, i.e., crystallinity of surface region of natural graphite samples would be an important structural factor influencing SEI formation. X-ray diffraction patterns shown in Fig. 1 and d_{002} values of natural graphite samples indicate that crystallinity of these three samples are similar to each other.

Table 3
R-values ($=I_D/I_G$) calculated from peak intensity ratios of Raman spectra

Graphite sample	Original	Plasma-fluorinated
NG5μm	0.24	0.27
NG10μm	0.25	0.33
NG15μm	0.26	0.39

Table 4
BET surface areas of plasma-fluorinated natural graphite samples

Graphite sample	Original (m^2 g^{-1})	Plasma-fluorinated (m^2 g^{-1})
NG5μm	13.6	12.3
NG10μm	9.0	7.2
NG15μm	7.0	5.9

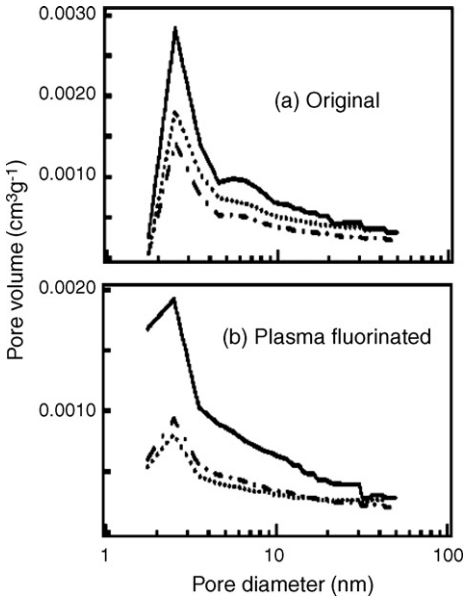

Fig. 3. Meso-pore size distribution of original and surface-fluorinated natural graphite samples. (a) original, (b) plasma-fluorinated ((—) NG5μm, (···) NG10μm, (–·–) NG15μm).

R-values obtained from Raman spectra are also nearly the same for all natural graphite samples, which means that surface disorder is almost the same for three natural graphite samples. This result suggests that there is no large difference in the rates of SEI formation by the decomposition of PC per unit surface area of three natural graphite samples if an actual current density is the same. Therefore difference in the surface areas should be taken into account for the electrochemical decomposition of PC. Fig. 4 shows first charge/discharge potential curves, and charge capacities and coulombic efficiencies as a function of cycle number for original and plasma-fluorinated natural graphite samples, obtained at 150 mA g^{-1}. In case of non-fluorinated samples, the longer potential plateaus at ca. 0.8 V indicating the reduction of PC were observed with increasing particle size, i.e., with decreasing surface area from NG5μm to NG15μm. First charge capacity decreased with decreasing surface area of natural graphite while first discharge capacity increased as given in Table 5. Therefore first coulombic efficiency of non-fluorinated sample highly diminished with decreasing surface area. As reported in a previous paper [40], the same samples gave high first coulombic efficiencies in EC-based solvent at 60 mA g^{-1} (NG5μm: 81.4%, NG10μm: 82.2%, NG15μm:

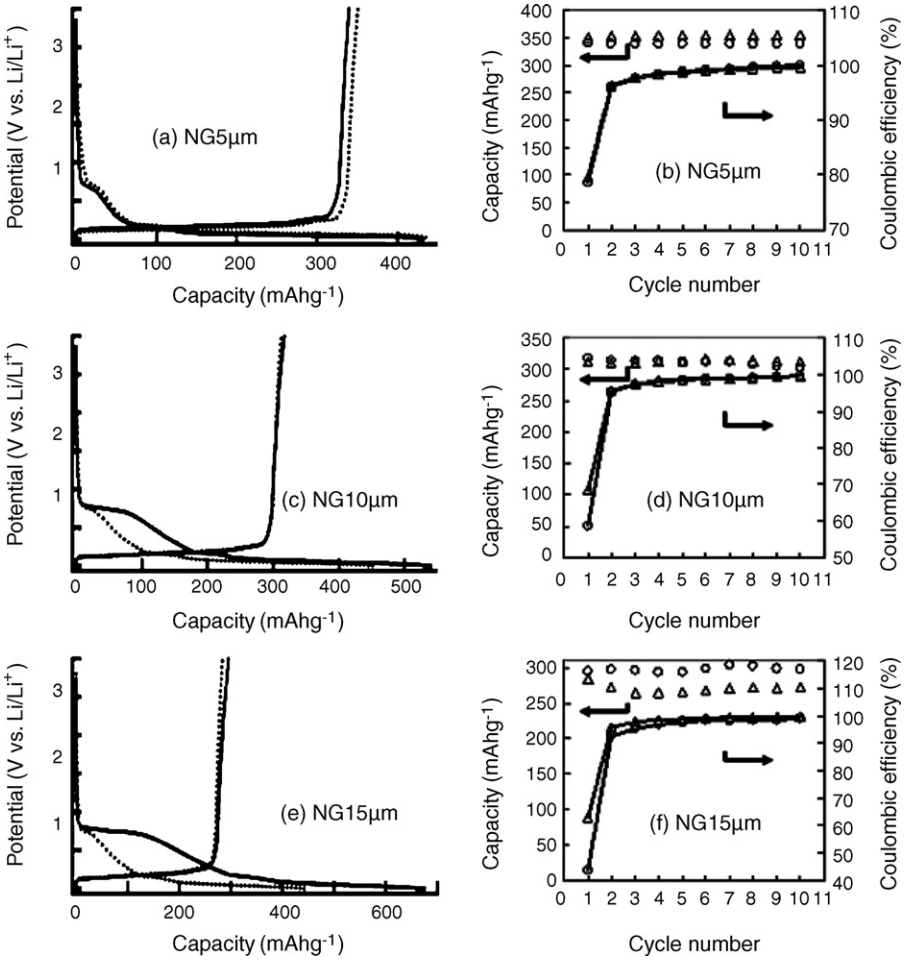

Fig. 4. First charge/discharge curves, charge capacities and coulombic efficiencies for original and surface-fluorinated natural graphite samples, obtained at 150 mA g^{-1} in 1 mol dm^{-3} $LiClO_4$–EC/DEC/PC (1:1:1 v/v/v): (a) and (b) NG5μm; (c) and (d) NG10μm; (e) and (f) NG15μm. ((—) original, (···) plasma-fluorinated (a), (c) and (e). (◯) original, (△) plasma-fluorinated (b), (d) and (f)).

Table 5
First charge/discharge capacities and first coulombic efficiencies for original and plasma-fluorinated natural graphite samples at 150 mA g^{-1}

Graphite sample	First discharge capacity (mAh g^{-1})	First charge capacity (mAh g^{-1})	First coulombic efficiency (%)
Original			
NG5μm	432	340	78.7
NG10μm	540	317	58.7
NG15μm	675	295	43.7
Fluorinated			
NG5μm	440	351	79.6
NG10μm	455	312	68.5
NG15μm	450	283	63.0

85.4%). The results show that decomposition of EC is reduced with decreasing surface area in EC-based solvent, indicating that SEI is quickly formed by decomposition of a small amount of EC. However, the decomposition of PC increased with decreasing surface area as shown in Fig. 4 and Table 5. The area of edge plane, where desolvation of PC and reduction of PC and Li^+ ion, followed by Li insertion may mainly occur, decreases with decreasing total surface area, i.e., from NG5μm to NG15μm. In addition, the ratio of edge plane to total surface area is high in fine graphite powder such as NG5μm (≈50%), but decreases with decreasing total surface area. Actual current density therefore increases with decreasing area of edge plane, that is, from NG5μm to NG15μm. Since SEI formation on high crystalline graphite is more difficult in PC-based solvent than in EC-based one, decomposition of PC would be accelerated with decrease in the area of edge plane, that is, with increase in actual current density. First coulombic efficiencies for NG5μm were high in both EC- and PC-containing solvents because NG5μm has the largest area of edge plane among three natural graphite samples, which may promote the smooth formation of SEI on NG5μm even in PC-containing solvent.

Effect of plasma-fluorination varied depending on the average particle size of natural graphite. NG5μm with the largest surface area showed almost the same charge/discharge behavior before and after fluorination as shown in Fig. 4(a) and (b) and Table 5 probably because the increase in *R*-value, i.e., surface disorder and decrease in surface area by surface fluorination were very small as given in Tables 3 and 4. Effect of plasma-fluorination was found in NG10μm and NG15μm with relatively smaller surface areas. Large potential plateaus at ca. 0.8 V indicating decomposition of PC were highly reduced on plasma-fluorinated NG10μm and NG15μm as shown in Fig. 4(c) and (e). First discharge capacities for NG10μm and NG15μm decreased to 455 and 450 mAh g^{-1} similar to that of NG5μm, 440 mAh g^{-1} by plasma-fluorination (Table 5). As a consequence, first coulombic efficiencies for NG10μm and NG15μm increased from 58.7 and 43.7% to 68.5 and 63.0%, i.e., the increments of first coulombic efficiencies were 9.7 and 19.3%, respectively, as given in Table 5. When the same natural graphite samples were fluorinated by F_2 at 200 °C and 300 °C, first coulombic efficiencies were 70.3 and 71.9% for NG10μm and 66.0 and 64.0% for NG15μm at 150 mA g^{-1} [40]. The increments of first coulombic efficiencies were 11.6–13.2% and 20.3–22.3% for NG10μm and NG15μm, which are only slightly larger than 9.7 and 19.3% obtained in the present study. This may be due to the difference in *R*-values between plasma-fluorination using CF_4 and fluorination with F_2. *R*-values of plasma-fluorinated NG10μm and NG15μm were similar to those obtained for the same graphites fluorinated by F_2 at 200 °C, but smaller than those obtained for the samples fluorinated at 300 °C [40]. Plasma-fluorination reduced surface areas as given in Table 4 while fluorination of the same natural graphites by F_2 increased surface areas [40]. Decrease in the surface areas may increase actual current density leading to increase in electrochemical decomposition of PC. However, first discharge capacities for plasma-fluorinated samples given in Table 5 were nearly the same as those obtained for the same graphites fluorinated by F_2 [40]. This suggests that increase in small meso-pores with diameter of 1.5–2 nm by plasma-fluorination brought about the increase in actual area of edge plane, i.e., electrode area, leading to reduction of electrochemical decomposition of PC. Coulombic efficiencies soon approached 100% after 1st cycle for all samples and cycleability was good except plasma-fluorinated NG15μm. Decrease in charge capacity of plasma-fluorinated NG15μm with cycling may arise from slight reduction of electrical contact with copper current collector due to expansion and shrinking of graphite by intercalation and deintercalation of Li^+ ions.

4. Conclusions

Plasma-fluorination of natural graphite powder samples with average particle sizes of 5 μm, 10 μm and 15 μm (NG5μm, NG10μm and NG15μm) was performed to prepare natural graphites with high surface disorder, and charge/discharge properties of plasma-fluorinated samples were investigated in 1 mol dm^{-3} $LiClO_4$–EC/DEC/PC (1:1:1 v/v/v). Electrochemical decomposition of PC increased with increasing particle size, i.e., with decreasing surface area of edge plane of non-fluorinated sample probably due to increase in actual current density. Plasma-fluorination increased surface disorder of three natural graphite samples though surface areas were reduced by radical reaction having surface etching effect. Fluorine contents in fluorinated graphite samples were small, 0.3–0.6 at.%, and surface fluorine concentrations were in the range of 14.8–17.3 at.%. Plasma-fluorination highly reduced the electrochemical decomposition of PC on NG10μm and NG15μm. As a consequence, first coulombic efficiencies for plasma-fluorinated NG10μm and NG15μm increased by 9.7 and 19.3% at 150 mA g^{-1}, respectively.

Acknowledgements

The present study was partly supported by a grant of the Frontier Research Project (continuation), "Materials for the 21st century—Development of novel device based on fundamental research of materials development for environment, energy and information" (for 2007–2009 fiscal years) from Ministry of education, culture, sports, science and technology. The authors

thank SEC Carbon Co. Ltd., for their kind supply of natural graphite samples used in the present study.

References

[1] R. Fong, U. von Sacken, J.R. Dahn, J. Electrochem. Soc. 137 (1990) 2009.
[2] T. Nakajima, H. Groult (Eds.), Fluorinated Materials for Energy Conversion, Elsevier, Oxford, 2005.
[3] T. Takamura, Bull. Chem. Soc. Jpn. 75 (2002) 21.
[4] L.J. Ning, Y.P. Wu, S.B. Fang, E. Rahm, R. Holze, J. Power Sources 133 (2004) 229.
[5] H. Wang, M. Yoshio, J. Power Sources 93 (2001) 123.
[6] S. Soon, H. Kim, S.M. Oh, J. Power Sources 94 (2001) 68.
[7] M. Yoshio, H. Wang, K. Fukuda, Y. Hara, Y. Adachi, J. Electrochem. Soc. 147 (2000) 1245.
[8] H. Wang, M. Yoshio, T. Abe, Z. Ogumi, J. Electrochem. Soc. 149 (2002) A499.
[9] M. Yoshio, H. Wang, K. Fukuda, T. Umeno, N. Dimov, Z. Ogumi, J. Electrochem. Soc. 149 (2002) A1598.
[10] Y.-S. Han, J.-Y. Lee, Electrochim. Acta 48 (2003) 1073.
[11] Y. Ohzawa, M. Mitani, T. Suzuki, V. Gupta, T. Nakajima, J. Power Sources 122 (2003) 153.
[12] Y. Ohzawa, M. Mitani, J. Li, T. Nakajima, Mater. Sci. Eng. B 113 (2004) 91.
[13] Y. Ohzawa, Y. Yamanaka, K. Naga, T. Nakajima, J. Power Sources 146 (2005) 125.
[14] R. Takagi, T. Okubo, K. Sekine, T. Takamura, Electrochemistry 65 (1997) 333.
[15] T. Takamura, K. Sumiya, J. Suzuki, C. Yamada, K. Sekine, J. Power Sources 81/82 (1999) 368.
[16] Y. Wu, C. Jiang, C. Wan, E. Tsuchida, Electrochem. Commun. 2 (2000) 626.
[17] S.-S. Kim, Y. Kadoma, H. Ikuta, Y. Uchimoto, M. Wakihara, Electrochem. Solid State Lett. 4 (2001) A109.
[18] J.K. Lee, D.H. Ryu, J.B. Ju, Y.G. Shul, B.W. Cho, D. Park, J. Power Sources 107 (2002) 90.
[19] I.R.M. Kottegoda, Y. Kadoma, H. Ikuta, Y. Uchimoto, M. Wakihara, Electrochem. Solid State Lett. 5 (2002) A275.
[20] I.R.M. Kottegoda, Y. Kadoma, H. Ikuta, Y. Uchimoto, M. Wakihara, J. Electrochem. Soc. 152 (2005) A1595.
[21] E. Peled, C. Menachem, D. Bar-Tow, A. Melman, J. Electrochem. Soc. 143 (1996) L4.
[22] J.S. Xue, J.R. Dahn, J. Electrochem. Soc. 142 (1995) 3668.
[23] Y. Ein-Eli, V.R. Koch, J. Electrochem. Soc. 144 (1997) 2968.
[24] Y. Wu, C. Jiang, C. Wan, E. Tsuchida, J. Mater. Chem. 11 (2001) 1233.
[25] Y.P. Wu, C. Jiang, C. Wan, Holze, Electrochem. Commun. 4 (2002) 483.
[26] Y. Wu, C. Jiang, C. Wan, R. Holze, J. Power Sources 111 (2002) 329.
[27] Y.P. Wu, C. Jiang, C. Wan, R. Holze, J. Appl. Electrochem. 32 (2002) 1011.
[28] T. Nakajima, M. Koh, R.N. Singh, M. Shimada, Electrochim. Acta 44 (1999) 2879.
[29] V. Gupta, T. Nakajima, Y. Ohzawa, H. Iwata, J. Fluorine Chem. 112 (2001) 233.
[30] T. Nakajima, V. Gupta, Y. Ohzawa, H. Iwata, A. Tressaud, E. Durand, J. Fluorine Chem. 114 (2002) 209.
[31] T. Nakajima, V. Gupta, Y. Ohzawa, M. Koh, R.N. Singh, A. Tressaud, E. Durand, J. Power Sources 104 (2002) 108.
[32] H. Groult, T. Nakajima, L. Perrigaud, Y. Ohzawa, H. Yashiro, S. Komaba, N. Kumagai, J. Fluorine Chem. 126 (2006) 1111.
[33] T. Nakajima, J. Li, K. Naga, K. Yoneshima, T. Nakai, Y. Ohzawa, J. Power Sources 133 (2004) 243.
[34] J. Li, K. Naga, Y. Ohzawa, T. Nakajima, A.P. Shames, A.I. Panich, J. Fluorine Chem. 126 (2005) 265.
[35] J. Li, Y. Ohzawa, T. Nakajima, H. Iwata, J. Fluorine Chem. 126 (2005) 1028.
[36] K. Naga, T. Nakajima, Y. Ohzawa, B. Žemva, Z. Mazej, H. Groult, J. Electrochem. Soc. 154 (2007) A347.
[37] K. Naga, T. Nakajima, S. Aimura, Y. Ohzawa, B. Žemva, Z. Mazej, H. Groult, A. Yoshida, J. Power Sources 167 (2007) 192.
[38] T. Nakajima, S. Shibata, K. Naga, Y. Ohzawa, A. Tressaud, E. Durand, H. Groult, F. Warmont, J. Power Sources 168 (2007) 265.
[39] K. Matsumoto, J. Li, Y. Ohzawa, T. Nakajima, Z. Mazej, B. Žemva, J. Fluorine Chem. 127 (2006) 1383.
[40] T. Achiha, T. Nakajima, Y. Ohzawa, J. Electrochem. Soc. 154 (2007) A827.
[41] S. Kuwabata, N. Tsumura, S. Goda, C.R. Martin, H. Yoneyama, J. Electrochem. Soc. 145 (1998) 1415.
[42] M. Gaberscek, M. Bele, J. Drofenik, R. Dominko, S. Pejovnik, Electrochem. Solid State Lett. 3 (2000) 171.
[43] J. Drofenik, M. Gaberscek, R. Dominko, M. Bele, S. Pejovnik, J. Power Sources 94 (2001) 97.
[44] M. Bele, M. Gaberscek, R. Dominko, J. Drofenik, K. Zupan, P. Komac, K. Kocevar, I. Musevic, S. Pejovnik, Carbon 40 (2002) 1117.
[45] M. Gaberscek, M. Bele, J. Drofenik, R. Dominko, S. Pejovnik, J. Power Sources 97/98 (2001) 67.
[46] B. Veeraraghavan, J. Paul, B. Haran, B. Popov, J. Power Sources 109 (2002) 377.
[47] M. Holzapfel, H. Buqa, F. Krumeich, P. Novak, F.M. Petrat, C. Veit, Electrochem. Solid State Lett. 8 (2005) A516.
[48] S. Rozen, C. Gal, Tetrahedron Lett. 25 (1984) 449.
[49] S. Rozen, C. Gal, J. Fluorine Chem. 27 (1985) 143.
[50] M. Koh, H. Yumoto, H. Higashi, T. Nakajima, J. Fluorine Chem. 97 (1999) 239.